RSC Advances

PAPER

View Article Online
View Journal | View Issue

Check for updates

Cite this: *RSC Adv.*, 2020, **10**, 32821

Cu(II)-alginate-based superporous hydrogel catalyst for click chemistry azide–alkyne cycloaddition type reactions in water†

Lahoucine Bahsis, *[ab] El-Houssaine Ablouh, *[cd] Hafid Anane,[b] Moha Taourirte,[c] Miguel Julve[e] and Salah-Eddine Stiriba[be]

A novel sustainable hydrogel catalyst based on the reaction of sodium alginate naturally extracted from brown algae *Laminaria digitata* residue with copper(II) was prepared as spherical beads, namely Cu(II)-alginate hydrogel (Cu(II)-AHG). The morphology and structural characteristics of these beads were elucidated by different techniques such as SEM, EDX, BET, FTIR and TGA analysis. Cu(II)-AHG and its dried form, namely Cu(II)-alginate (Cu(II)-AD), are relatively uniform with an average pore ranging from 200 nm to more than 20 μm. These superporous structure beads were employed for the copper catalyzed [3 + 2] cycloaddition reaction of aryl azides and terminal aryl alkynes (CuAAC) *via* click chemistry at low catalyst loading, using water as a solvent at room temperature and pressure. The catalytic active copper(I) species was generated by the reduction of copper(II) by terminal alkyne *via* the oxidative alkyne homocoupling reaction. The prepared catalysts were found to be efficient (85–92%) and regioselective by affording only 1,4-disubstituted-1,2,3-triazoles. They were also recoverable and reused in their dried form for at least four consecutive times without a clear loss of efficiency. A mechanistic study was performed through density functional theory (DFT) calculations in order to explain the regioselectivity outcome of Cu(II)-alginate in CuAAC reactions. The analysis of the local electrophilicity (ω_k) at the electrophilic reagent and the local nucleophilicity (N_k) at the nucleophilic confirms the polar character of CuAAC. This catalyst has the main advantage of being sustainably ligand-free and recyclable.

Received 23rd July 2020
Accepted 18th August 2020

DOI: 10.1039/d0ra06410f

rsc.li/rsc-advances

Open Access Article. Published on 03 September 2020. Downloaded on 2/9/2026 1:57:27 PM.
This article is licensed under a Creative Commons Attribution-NonCommercial 3.0 Unported Licence.

1. Introduction

In modern drug research technology, the synthesis of most active organic molecules is necessitated in short time and efficient manner, under mild conditions. Click chemistry is one of the modern concepts based on chemical reactions that take place with high yields and high regio- and stereo-selectivity outcome, in low reaction time, affording new carbon-heteroatom and carbon–carbon bonds.[1] The most representative and popular click chemistry reaction is the copper catalyzed [3 + 2] cycloaddition reaction of azides and alkynes (CuAAC).[2,3] This synthetic methodology is now considered an aesthetic and convenient route for the regioselective synthesis of 1,4-disubstituted-1,2,3-triazoles from simple and structurally diversified starting materials.[4–6] In fact, 1,2,3-triazole derivatives are known by their application in biorthogonal chemistry,[7] material science,[8] and medicinal chemistry.[9–14] In addition, they are important because of their application as precursors for the preparation of mesoionic carbenes (MICs), suitable employment in the preparation of metal complexes with several metal ions (Au, Ag, Ir, Rh, and Ru), and their use in transition-metal-mediated catalysis.[15–19]

In the context of designing and preparing copper catalysts for CuAAC, a variety of homogenous and heterogeneous catalytic systems were used for the selective synthesis of 1,4-disubstituted-1,2,3-triazoles.[20–26] Taking into account the green chemistry principles, the quest for heterogeneous catalysts for CuAAC has led to several cheap, facile and reusable catalysts.[27,28] In addition, the immobilization of metal catalysts on biocompatible supports is one of the best methods to improve efficiency, recovery and sustainability of catalysts.[29–32]

The great interest in setting-up sustainable catalysts leads to the use of naturally occurring polymers such as alginate because of their low cost, chemical stability, biocompatibility, and biodegradability.[33] This biopolymer constitutes an excellent

[a]*Département de Chimie, Faculté des Sciences d'El Jadida, Université Chouaïb Doukkali, B.P.: 20, 24000 El Jadida, Morocco. E-mail: bahsis.lahoucine@gmail.com*
[b]*Laboratoire de Chimie Analytique et Moléculaire, LCAM, Faculté Polydisciplinaire de Safi, Université Cadi Ayyad, 4162 Safi, Morocco*
[c]*Laboratoire de Chimie Bioorganique et Macromoléculaire, Faculté des Sciences et Techniques de Marrakech, Université Cadi Ayyad, 40000 Marrakech, Morocco. E-mail: lhoussainiblah@gmail.com*
[d]*Centre d'Analyse et de Caractérisation, Université Cadi Ayyad, 40000 Marrakech, Morocco*
[e]*Instituto de Ciencia Molecular/ICMol, Universidad de Valencia, C/Catedrático José Beltrán, 46980, Paterna, Valencia, Spain*

† Electronic supplementary information (ESI) available. See DOI: 10.1039/d0ra06410f

Open Access Article. Published on 03 September 2020. Downloaded on 2/9/2026 1:57:27 PM.
This article is licensed under a Creative Commons Attribution-NonCommercial 3.0 Unported Licence.

polymeric backbone for the coordination of copper(II) and other transition metal ions due to the presence of functional groups in their structure, which act as donors towards metal ions. In addition, the sodium alginate biopolymer is characterized by a broad chemical modification capacity and a high surface area, making it an interesting biodegradable polymer to support metal catalysts.[34,35] In line with their application in technological fields such as agriculture, tissue engineering and drug delivery, superporous hydrogels (SPHs) may constitute excellent supports for the heterogenization of catalysts.[36,37]

As a continuation of our research efforts in designing and preparing sustainable catalysts in click chemistry,[38–40] we now report the preparation of a superporous hydrogel bead-based catalyst for CuAAC through the coordination of copper(II) to a naturally-occurring alginate biopolymer. The resulting Cu(II)-alginate hydrogel bead catalytic system exhibits high activity and regioselectivity for the click chemistry of 1,4-disubstituted-1,2,3-triazoles in aqueous solution at room temperature. Its recovery/recyclability was also evaluated. Additionally, Density Functional Theory (DFT) calculations were performed to account for the regioselectivity outcome of this catalyst in the CuAAC-type reaction.

2. Experimental

2.1. Materials and methods

Sodium alginate was obtained from Moroccan *Laminaria digitata* brown seaweed according to the procedures detailed elsewhere.[41] Copper(II) chloride (99.0%) was purchased from Analar Normapur. All other abovementioned reagents were purchased from Sigma-Aldrich, Alfa Aesar and Acros, and were used as provided by the manufacturer without any further purification. Thin-layer chromatography (TLC) plates (Merck Kieselgel 60 F254) were used to monitor the reactions, and they were observed under UV light at 254 nm. A Bruker DRX-300 Avance spectrometer was used to record the ^{1}H and ^{13}C NMR spectra using $CDCl_3$ as the solvent. An electrothermal 9100 apparatus measured the melting points.

The surface morphology of the Cu-alginate catalyst was conducted using TESCAN-VEGA3 SEM at an accelerating voltage of 20 kV. An energy-dispersive X-ray (EDAX) analyser was employed to identify the specific elemental composition and mapping. The functional groups of sodium alginate and the Cu-alginate catalysts were analysed using FTIR (Bruker VERTEX 70), operating at 4 cm^{-1} over a range of 4000–400 cm^{-1}. The thermal properties of the prepared catalyst were also studied using thermogravimetric analysis (TA-TGA55). Atomic absorption spectroscopy (Aurora AI800) was used to determine the copper loading.

2.2. Preparation of the Cu(II)-alginate hydrogels

Sodium alginate solution was prepared by pouring 2.0 g of sodium alginate into 200 mL of deionized water with stirring for 2 hours to obtain a homogeneous gel solution. The Cu(II)-alginate beads were prepared by using a syringe pump with a flow rate of 15 mL h^{-1}. Then, the sodium alginate solution was added dropwise into a solution of $CuCl_2$ (0.1 M) under slow stirring at 25 °C. The fast complex formation between the copper(II) ions and the carboxylate groups on the surface of the sodium alginate polymer led to freezing the spherical beads of the drop within the solution. Afterwards, the obtained spherical beads were allowed to stand in the copper(II) solution for 24 hours. After maturation time, the beads were washed several times with deionized water. The loading amount of copper(II) was measured using atomic absorption spectrometry, and it was found to be 9.35% (w/w). The catalytic applications were immediate in the case of the Cu(II)-alginate hydrogel beads (Cu-AHG) or dried bead form using a freeze dryer (Cu-AD).

2.3. Characterization

2.3.1. Specific surface area measurement. The surface area of the Cu(II)-alginate hydrogel beads was measured using a surface area analyzer (Micromeritics, ASAP 2010) at 77 K. Samples were degassed at 120 °C for 24 h under nitrogen flow to remove the moisture adsorbed on the solid surface. The monopoint BET method was used to evaluate the specific surface area (S_{BET}).

2.3.2. Swelling experiments. The swelling ratio (Q_m), corresponding to the change in mass of the prepared Cu(II)-alginate hydrogel beads in water at 25 °C, was calculated using eqn (1):

$$Q_m = \frac{W_s}{W_d} \quad (1)$$

where W_s and W_d are the initial weights of the wet and dried beads, respectively. Briefly, the dry beads were pre-weighed (0.1 ± 0.001 g) and then immersed in 100 mL of deionized water. The weight of the wet beads was recorded after 10 h.

2.4. General experimental methods for the synthesis of 1,4-triazoles

Azide (0.6 mmol) and alkyne derivatives (0.5 mmol) and 2 mol% of Cu(II)-alginate beads were placed in a reaction tube, and 3 mL of deionized water was added. The reaction tube was placed on a magnetic stirring plate at room temperature. After completion as determined by TLC, the reaction mixture was diluted with diethyl ether. Then, the catalyst was recovered by simple filtration. The diethyl ether solvent phase was removed under vacuum to afford the pure product, which was purified by recrystallization if needed. The recovered catalyst was dried and reused at least four times without losing its activity.

2.5. Computational methods

The optimizations of the geometries were performed using the Perdew and Wang function (PW91) as implemented in the DmoL^3 code.[42–44] The d-polarization included basis set (DNP) was employed, which is comparable to that of Pople's 6-31G(d,p) basis set, and used an effective core potential (ECP) for the copper atoms.[45,46] The adsorption energies (E_{ads}) were defined by eqn (2):

$$E_{ads} = E_{\text{Cu-alginate+adsorbate}} - E_{\text{Cu-alginate}} - E_{\text{adsorbate}} \quad (2)$$

 This journal is © The Royal Society of Chemistry 2020

Open Access Article. Published on 03 September 2020. Downloaded on 2/9/2026 1:57:27 PM.
This article is licensed under a Creative Commons Attribution-NonCommercial 3.0 Unported Licence.

where $E_{\text{Cu-alginate}}$ and $E_{\text{adsorbate}}$ are the energies of Cu-alginate and free adsorbate, respectively. $E_{\text{Cu-alginate+adsorbate}}$ is the total energy of the adsorbate on the Cu-alginate. The effect of the solvent (water) on the E_{ads} of all intermediates was also studied at the same level of theory using the conductor-like screening model (COSMO) implemented in DMol^3.[47]

The global electrophilicity (ω) and nucleophilicity (N) indexes were measured at the same level, and are given by the following simple expressions: $\omega = \mu^2/2\eta$ and $N = E_{\text{H}}$ (our molecule or complex) $- E_{\text{H}}$ (tetracyanoethylene (TCE)).[48,49] The values of the energy of the frontier molecular orbitals HOMO and LUMO, E_{H} and E_{L}, were calculated to identify the electronic chemical potential μ and chemical hardness η using the expressions $\mu = (E_{\text{H}} + E_{\text{L}})/2$ and $\eta = (E_{\text{L}} - E_{\text{H}})$, respectively. The local reactivity index was calculated using the Fukui function implemented in DMol^3 (see ESI for more information†).[50]

3. Results and discussion

3.1. Characterization of the Cu(II)-alginate hydrogel beads

The surface and chemical structural properties of the prepared Cu(II)-alginate hydrogel beads were examined by BET, SEM, EDX, TGA and FTIR analysis. Aqua spherical beads were obtained by the crosslinking process of sodium alginate (SA) with Cu^{2+}. After the freeze-drying step, the resulting material consisted of blue coloured beads. Digital images of the Cu-AHG and Cu-AD beads were taken to determine their mean diameter by the least-squares method, allowing us to draw up a histogram that reflected the distribution of the beads (Fig. 1). The comparison of the mean size beads was done by calculating the average diameter whose values were 2.75 and 2.82 mm for the Cu-AHG and Cu-AD beads, respectively. These results indicate that the difference is significant, a feature that is probably due to the freeze-drying process. The stability of the cross-linked alginate hydrogels beads was greater at pH values below 7, and also in the absence of univalent cations such as K^+ and Na^+, which can be involved in ion exchange with copper.[51,52]

More specifically, the scanning electron micrographs of dried copper(II)-alginate (Cu-AD) beads in the dry state show a similar size, and kept their spherical shape with porous structures. In addition, SEM images of the surface beads show a relatively smooth surface, and had a regular homogeneous shape with some wrinkles and pores (Fig. 2a and b). The morphological analysis of the bead section shows a porous structure. As one can observe at high magnification (Fig. 2d), cross-linked copper-alginate forms a porous structure that can be related to an abundant porosity. The pore sizes are relatively uniform with an average pore ranging from 200 nm to more than 20 μm. A loose network of interconnected fibrils forms this superporous structure.[53] Therefore, the Cu(II)-AD catalyst presents an important macroporosity due to the removal of absorbed water in wet beads and the formation of extensively interconnected fibrils with the successful freeze-drying process and thus dry beads are obtained. On the other hand, the prepared Cu-AD beads were dried in freeze-drying conditions to achieve the corresponding aerogel catalyst with increased surface areas, which conferred effective catalytic properties. The surface area for Cu(II)-AD, examined using the BET method, was 261 $m^2\ g^{-1}$.

The swelling experiment was used as a simple and basic method to investigate the water uptake of the prepared hydrogels beads.[54] The result shows that the water-swelling ratio of the Cu(II)-alginate hydrogel beads was found to be 13.7 $g\ g^{-1}$ (the swelling ratio ($g\ g^{-1}$) was measured by dividing the weight of the swollen gel by the weight of the initial dried sample), relating to its high porosity and the more hydrophilic structure of alginate biopolymer. Furthermore, BET, swelling and microstructural analysis suggested that the Cu(II)-alginate hydrogel beads were more suitable for catalytic activity.

To confirm the successful cross-linking of the alginate polymer with copper(II) ions, the structures of the starting material (sodium alginate) and dried Cu(II)-alginate beads were examined by FTIR spectroscopy. It was also used to identify and compare the functional groups present in both materials (Fig. 3). The FTIR spectrum of sodium alginate and dried Cu(II)-alginate beads showed several peaks with the same wavenumber around 3435, 2929, 1414, 1030 and 882 cm^{-1}, corresponding to O–H antisymmetric stretching vibrations, C–H stretching vibrations, symmetric $-COO^-$ stretching vibrations, symmetric C–O–C stretching vibrations and C–H deformation

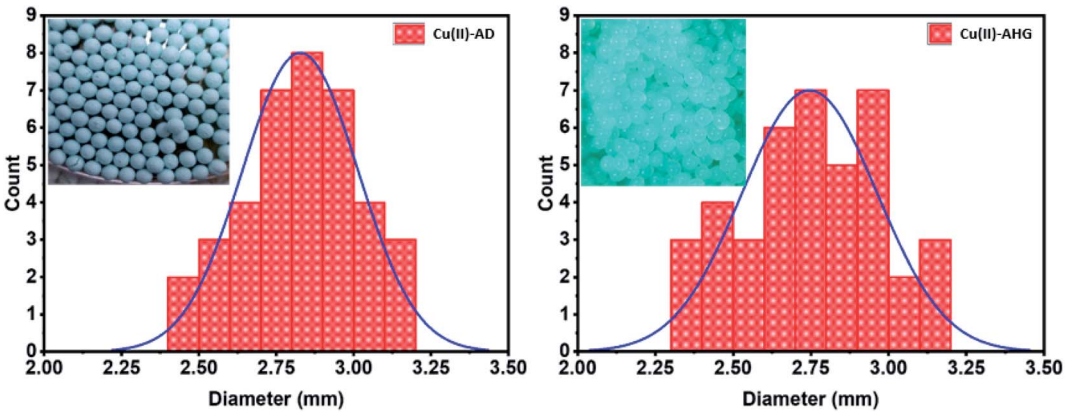

Fig. 1 Size distribution histograms determined from the digital images taken for the Cu–SA beads before (Cu-AHG) and after freeze-drying (Cu-AD).

Open Access Article. Published on 03 September 2020. Downloaded on 2/9/2026 1:57:27 PM.
This article is licensed under a Creative Commons Attribution-NonCommercial 3.0 Unported Licence.

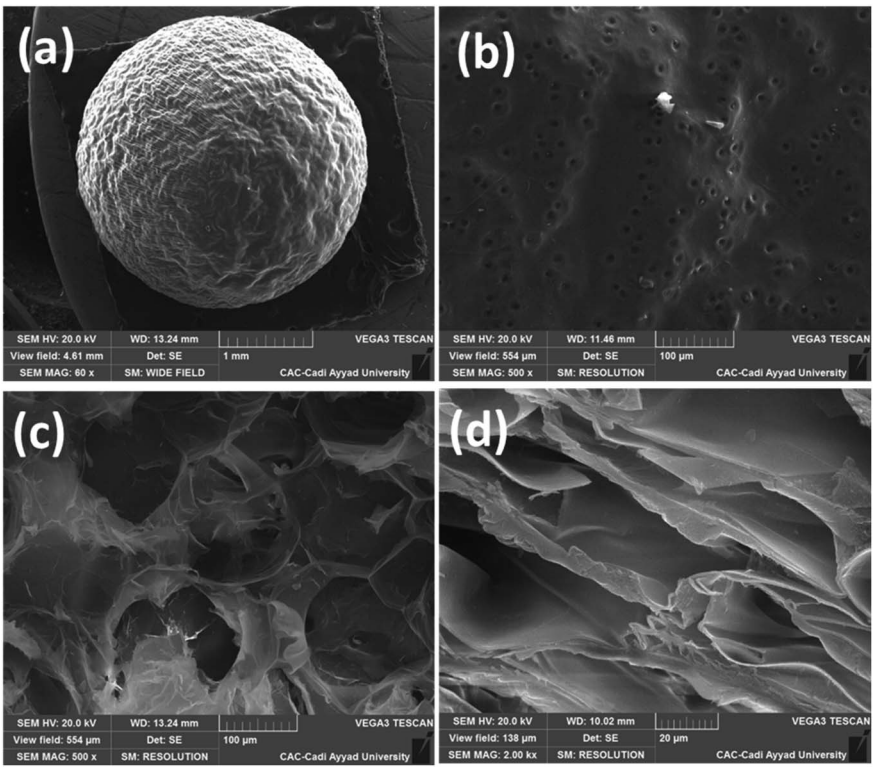

Fig. 2 SEM micrographs of the Cu(II)-AD bead surface (a and b) and Cu(II)-AD bead cross-section (c and d).

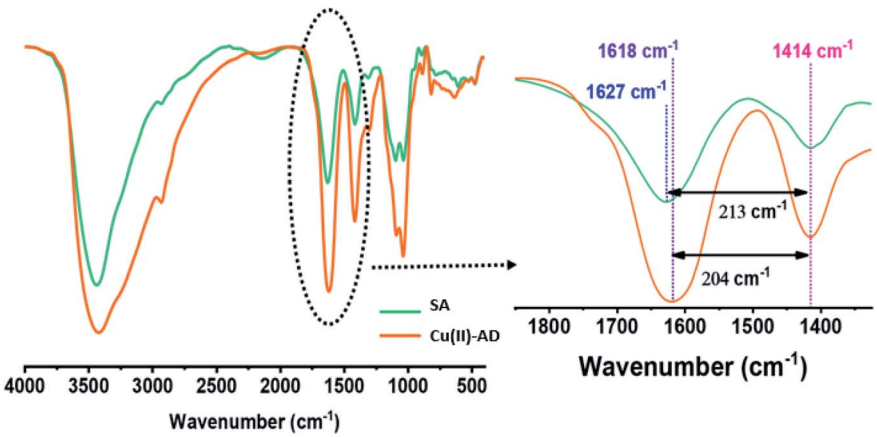

Fig. 3 FTIR spectra of sodium alginate (SA) and dried Cu(II)-alginate beads (Cu(II)-AD).

vibrations of the β-mannuronic acid residues, respectively, according to the literature data.[55,56]

After the cross-linking process with the copper(II) ions, the band assigned to the asymmetric elongation vibration of COO^- was significantly downshifted to 1618 cm^{-1}, confirming that the alginate chains interacted more effectively with copper(II) ions through a strong electrostatic attraction.[57] Additionally, the copper(II) ions act as cross-linking agents to form the beads because the guluronic units in the alginate polymers can capture divalent cations.[58] This interaction can be the consequence of the coordination with copper(II) ions forming superporous hydrogel beads (Scheme 1).

EDX analysis revealed that the Cu(II)-alginate beads were composed of C, O, and Cu atoms, which indicated that the copper element was successfully incorporated into the prepared material. Compared with the naturally-occurring sodium alginate used in this study, the Cu(II)-AD bead material does not contain any sodium atom due to the ion exchange with copper(II) ions during the cross-linking process.[59,60] In addition, we should note that the atomic ratio of copper on the surface of the bead (surface-section) was almost the same as that inside the bead (cross-section) (Fig. 4).

The distribution of copper is one of the main factors that affect the catalytic activity performance. To qualitatively

 This journal is © The Royal Society of Chemistry 2020

Open Access Article. Published on 03 September 2020. Downloaded on 2/9/2026 1:57:27 PM.
This article is licensed under a Creative Commons Attribution-NonCommercial 3.0 Unported Licence.

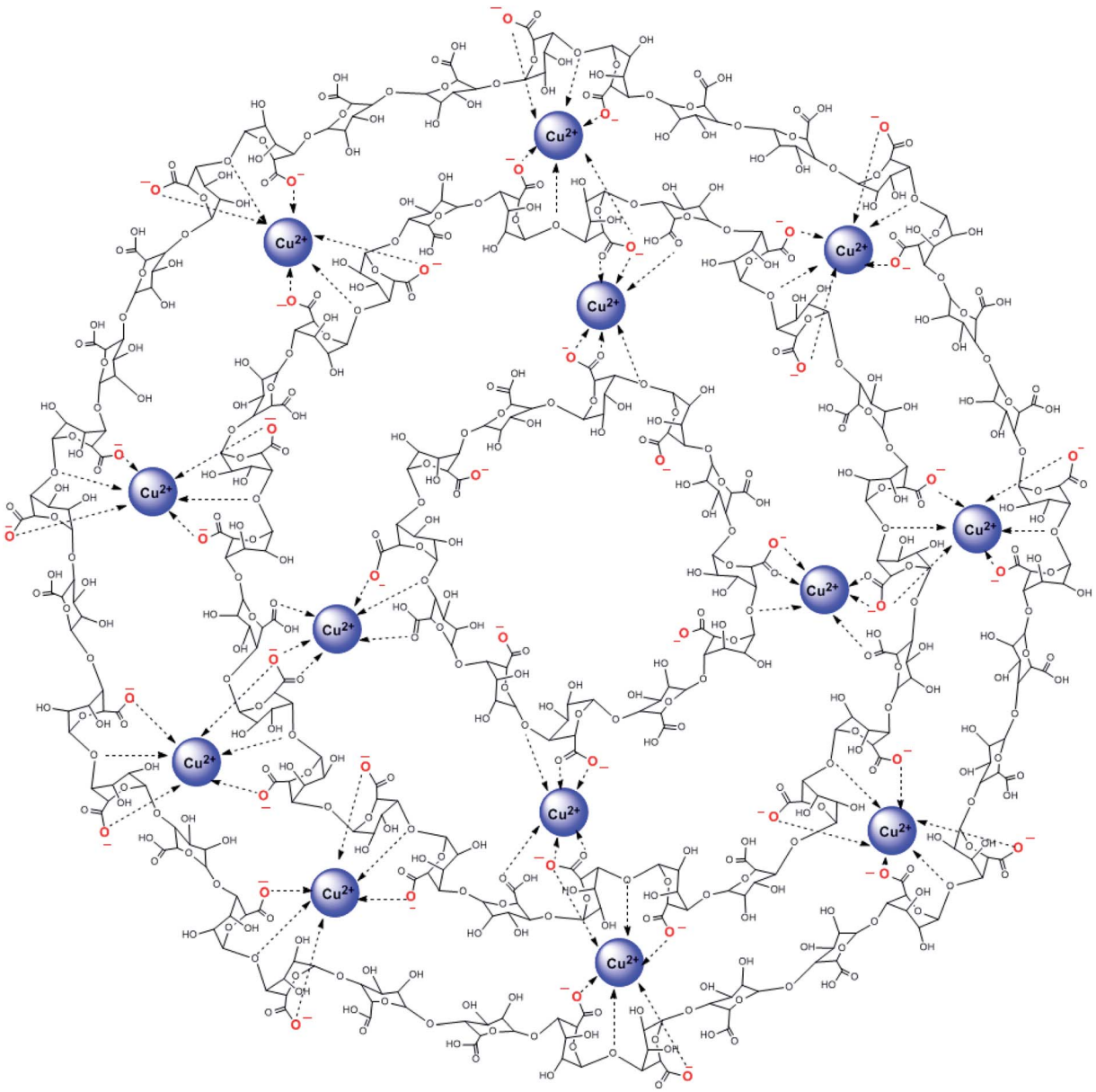

Scheme 1 Proposed structure of the cross-linked Cu(II)-alginate hydrogel beads.

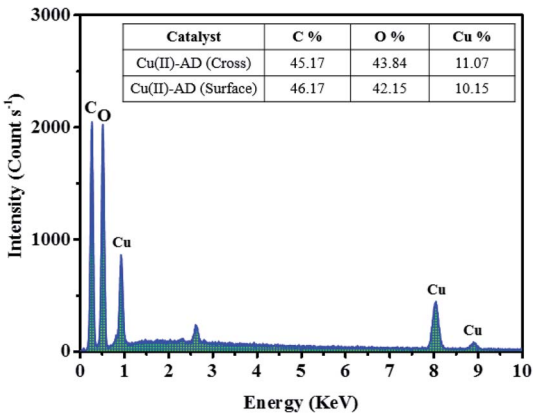

Fig. 4 EDX spectra and chemical composition of the Cu(II)-AD surface.

confirm the presence and good dispersion of the required elements, EDX mapping can help in determining the distribution of copper on the surface by analyzing the copper contents of the Cu(II)-AD bead material. The EDX mapping images show that the copper element is homogeneously distributed over the surface of the prepared bead material (Fig. 5). This suggests that these beads are good candidates for the copper catalyst reactions, as well as for the synthesis of 1,2,3-triazoles.

The thermal properties of sodium alginate (SA) and cross-linked alginate [Cu(II)-AD] were investigated by TGA analysis (Fig. 6). The presence of copper in the SA matrix should change the thermal behaviour of the gel, which could be identified by TGA. The analysis shows that the Cu-alginate beads are more stable than the sodium alginate polymer. About 10% of weight loss occurs in the first stage in the temperature range 50–200 °C

Open Access Article. Published on 03 September 2020. Downloaded on 2/9/2026 1:57:27 PM.
This article is licensed under a Creative Commons Attribution-NonCommercial 3.0 Unported Licence.

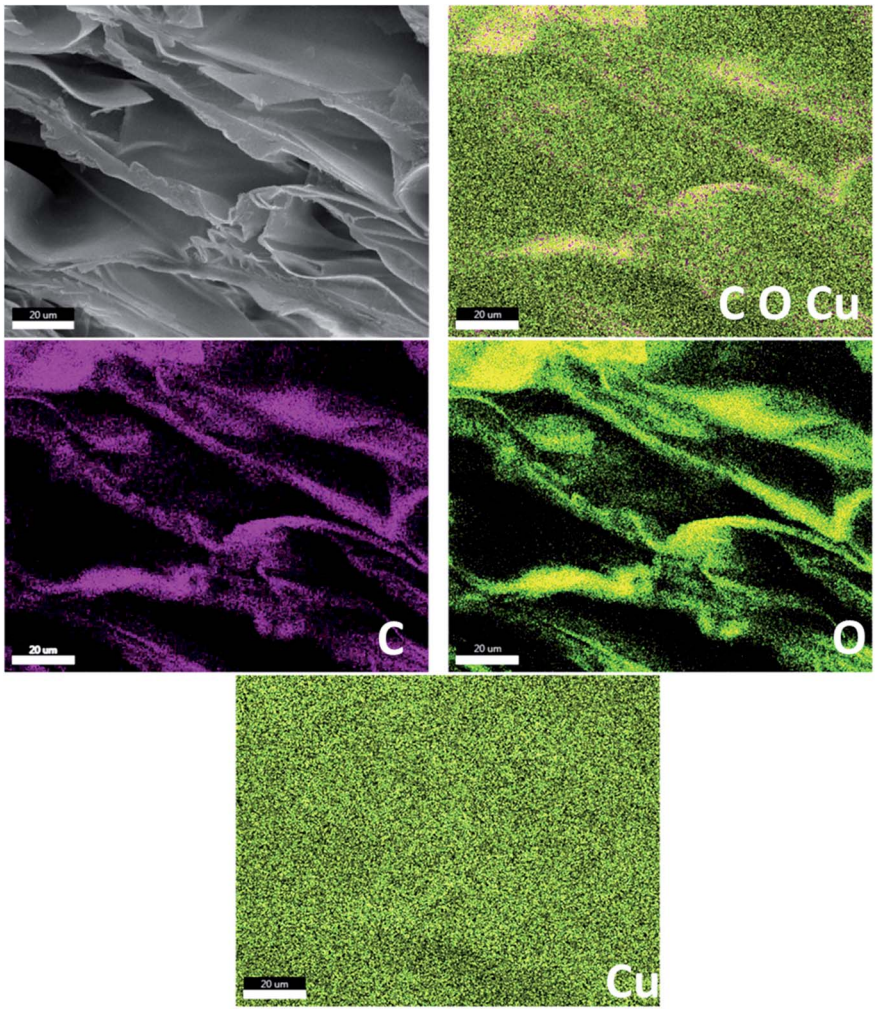

Fig. 5 Energy-dispersive X-ray mapping images of the Cu(II)-AD surfaces.

due to the evaporation of absorbed water present in the samples. The second stage (*ca.* 42% of mass loss) with a maximum at 240 °C is assigned to the removal of the side –OH groups of the alginate polymer by chain-stripping, leading to a polyene formation. Finally, the decomposition of carbonaceous materials would account for the last weight-loss stage (*ca.* 65%) at 350 °C.[61]

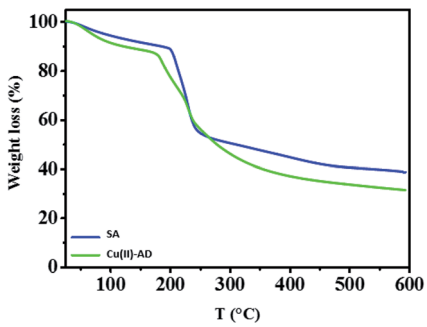

Fig. 6 TGA analysis of the sodium (SA) and cross-linked [Cu(II)-AD] alginates.

3.2. Catalytic activity

To investigate the catalytic activity of the prepared catalysts for click reactions, phenylacetylene (**1a**) and benzyl azide (**2a**) were selected as model substrates for the reaction using water as solvent at room temperature (Scheme 2). It was observed that the use of $CuSO_4$ only led to poor yields of the desired product (**3a**) at room temperature (Table 1). Importantly, both Cu(II)-alginate beads led to a regioselective synthesis of 1,4-disubstituted-1,2,3-triazole in a very good yield (98%) within 24 h for Cu(II)-AHG and 48 h for the dried Cu(II)-AD beads. The influence of the amount of the catalyst on the yield of the

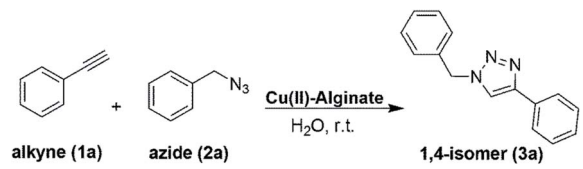

Scheme 2 Cu(II)-alginate bead catalyzed [3 + 2] cycloaddition reaction of benzyl azide and phenylacetylene.

 This journal is © The Royal Society of Chemistry 2020

Open Access Article. Published on 03 September 2020. Downloaded on 2/9/2026 1:57:27 PM.
This article is licensed under a Creative Commons Attribution-NonCommercial 3.0 Unported Licence.

Table 1 Optimization of the Cu(II)-alginate bead catalysts for the synthesis of 1,4-disubstituted-1,2,3-triazoles

Catalyst	Loading copper[a] (mol%)	Time (h)	Yield[b] (%)
$CuSO_4$	5	24	30
Cu(II)-AHG	0.5	24	33
	1	24	54
	1.5	24	68
	2	**24**	**95**
Cu(II)-AD	0.5	48	30
	1	48	41
	1.5	48	62
	2	**48**	**98**
	2.5	24	69

[a] (Loading of copper used for reaction/number of moles of alkyne) × 100. [b] Reaction conditions: benzyl azide (0.6 mmol), phenylacetylene (0.5 mmol), water (3 mL), Cu-catalyst, room temperature.

reaction was also investigated (Table 1). In the case of Cu(II)-AHG, the use of 2 mol% resulted in excellent yields after 24 h of reaction time and the decrease of catalyst loading decreased the yield of the reaction. The reaction in the presence of 2 mol% of Cu(II)-AD also led to excellent yields after 48 h (Table 1). Increasing the amount of Cu(II)-AD to 2.5 mol% [Cu] changed the yield and reaction times. However, upon further decreasing the amount of the Cu(II)-AD catalyst to 1 mol% [Cu], the rate of the reaction was reduced. Thus, we decided to use 2 mol% for both catalysts of Cu(II)-alginate beads for subsequent studies (Table 1). Once the optimum conditions for the CuAAC between phenylacetylene and benzyl azide of the copper(II)-supported alginate catalysts were determined, a variety of alkynes and azides were reacted using the Cu(II)-AHG and Cu(II)-AD beads as catalysts in water under mild conditions (Table 2). In all cases, the substituents (electron-rich, electron-withdrawing, and heterocycle) did not have any particular effect when using both catalysts, as most of the reactions were completed affording the corresponding 1,4-isomer 1,2,3-triazole in good to excellent yields (85–92%). It should be noted that the use of the Cu(II)-AHG beads as a catalyst in CuAAC gave excellent yields in most cases in 24 h, compared with the Cu(II)-AD beads that required almost 48 h to do so. This fact could be explained by the facile accessibility of both reactants into the Cu(II)-AHG beads. Most of the reactions can be monitored visually as the product

Table 2 [3 + 2] cycloaddition reaction of different alkyne derivatives with azides catalyzed with Cu(II)-alginate beads[a]

Entry	Alkyne	Azide	Product	Yield[b] (%)	Yield[c] (%)
1	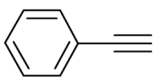	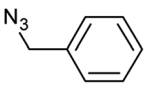	**3a**	93	90
2	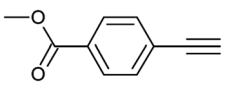	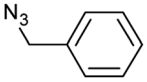	**3b**	90	92
3	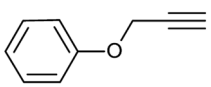	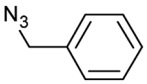	**3c**	96	90
4	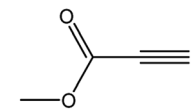	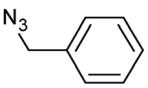	**3d**	97	88
5	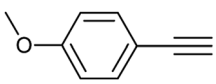	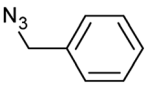	**3e**	94	94
6	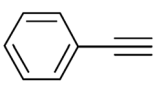	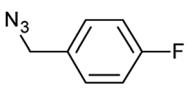	**3f**	96	90
7	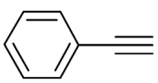	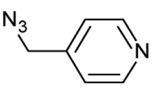	**3g**	96	89
8	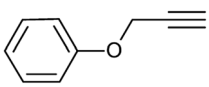	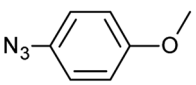	**3h**	96	85
9	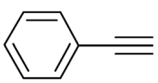	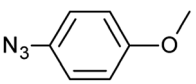	**3i**	95	92

[a] Reaction conditions: azide (0.6 mmol), alkyne (0.5 mmol), water (5 mL), catalyst (4 mg, 2 mol% Cu) at room temperature. [b] Isolated yield after 24 h for Cu(II)-AHG. [c] Isolated yield after 48 h for Cu(II)-AD.

Open Access Article. Published on 03 September 2020. Downloaded on 2/9/2026 1:57:27 PM.
This article is licensed under a Creative Commons Attribution-NonCommercial 3.0 Unported Licence.

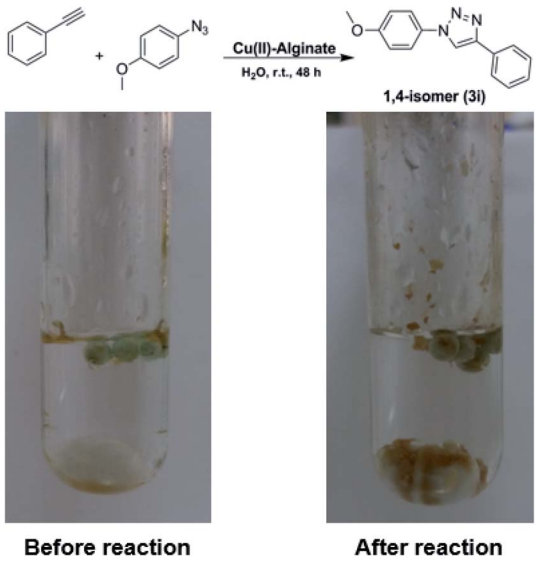

Fig. 7 Pictures of the reaction mixture before (left) and after (right) completion of the reaction using Cu(II)-AD beads.

crystallized out from the aqueous reaction media (Fig. 7). Moreover, all corresponding 1,2,3-triazoles were obtained in excellent yields in both cases, and the final product did not require any further purification by conventional methods.

In order to prove the efficiency of our catalytic system with respect to the other reported catalytic ones in the context of CuAAC, comparative results of the copper-catalyzed phenylacetylene (**1a**) and benzyl azide (**2a**) cycloaddition reaction chosen as model reaction are compiled in Table 3. The illustrated results show that Cu(II)-AHG and Cu(II)-AD are largely superior to the Cu(II)-alginate [as indicated by the catalyst turnover number (TON)], as well as to the Cu(II)-polyethylenimine and $CuSO_4$-PEG-PS systems. Similar to Cu(II/I)-cellulose, $CuSO_4$-chitosan and $CuSO_4$-cellulose-poly(hydroxamic acid) were observed in terms of their reactivity and sustainable reaction conditions. Remarkably, fCu(II)-AHG and its dried form (Cu(II)-AD) did not require external reducing reagents for the generation of the copper(I) species, and were easily separated from the final triazole products.

3.3. Mechanistic studies

To achieve a better understanding of the experimentally observed regioselectivity, Density Functional Theory (DFT) calculations were carried out by choosing an appropriate model of the Cu(II)-alginate catalysts, as illustrated in Scheme 3. First, the catalytic copper(I) species was generated by the reduction of copper(II) by the terminal alkyne *via* oxidative alkyne homocoupling reaction, known as the Glasser reaction.[67,68] The cycloaddition [3 + 2] azide–alkyne starts through the formation of the copper-acetylide complex by the *in situ* coordination of the terminal alkyne to the copper(I) species.[69–77] Furthermore, a six-membered copper-containing intermediate complex (IC) was formed in the presence of azides, which led a conducting path to the triazolide ring (AT) along with the Cu–C bond formation. Finally, the 1,4-disubstituted-1,2,3-triazole was formed under slightly acidic conditions from the triazolide ring, and the catalyst was regenerated (Scheme 3).[78]

Recently, the [3 + 2] cycloaddition azide–alkyne reactions (AAC) was analyzed using local reactive indexes defined in the context of conceptual DFT (CDFT), which showed that the analysis of the local electrophilicity (ω_k) at the electrophilic reagent and the local nucleophilicity (N_k) at the nucleophilic one were enabled for understanding the behaviour of polar cycloaddition.[79–81] Based on this, the Fukui functions were used to calculate the local electrophilicity and nucleophilicity of the

Table 3 Comparison of the click chemistry of 1,4-disubstituted-1,2,3-triazoles by our protocols with other catalytic methods

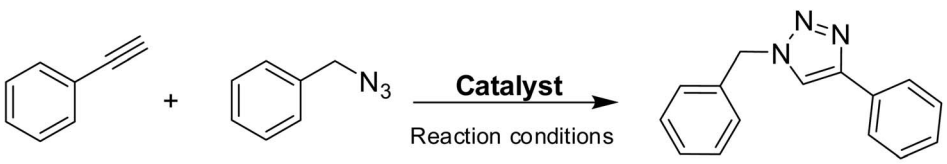

1a 2a 3a

Entry	Catalyst	[Cu] loading (mol%)	Conditions	Time (h)	Yield (%)	TON	Ref.
1	Cu(II)-AHG	2	H_2O, r.t.	24	95	24	This work
2	Cu(II)-AD	2	H_2O, r.t.	48	93	23	
3	Cu(II)-alginate	21	H_2O, r.t.	18	98	4.6	62
4	Cu(II)-cellulose	1.2	H_2O, r.t.	12	96	40	38
5	Cu(I)-cellulose	0.14	H_2O, r.t.	4	93	332	
6	Cu(II)-poly(hydroxamic acid)	0.1	H_2O, 50 °C	4	91	910	63
7	$CuSO_4$-chitosan	n.d.[a]	H_2O, r.t.	4	99	—	64
8	Cu(II)-polyethylenimine	5	H_2O, r.t.	24	98	12	65
9	$CuSO_4$-PEG-PS[b]	5	H_2O, N_2, r.t., sodium ascorbate (10 mol%)	12	97	9.7	66

[a] Not determined in mol%, given as $CuSO_4$-chitosan (5 mg). [b] PEG-PS: poly(ethylene glycol)-polystyrene.

 This journal is © The Royal Society of Chemistry 2020

Open Access Article. Published on 03 September 2020. Downloaded on 2/9/2026 1:57:27 PM.
This article is licensed under a Creative Commons Attribution-NonCommercial 3.0 Unported Licence.

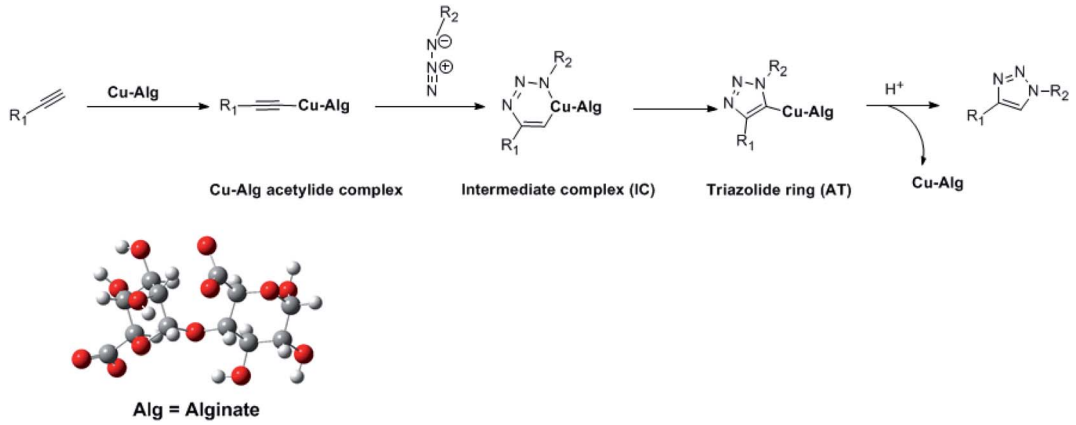

Scheme 3 Proposed mechanism of the CuAAC catalyzed by Cu-alginate catalysts.

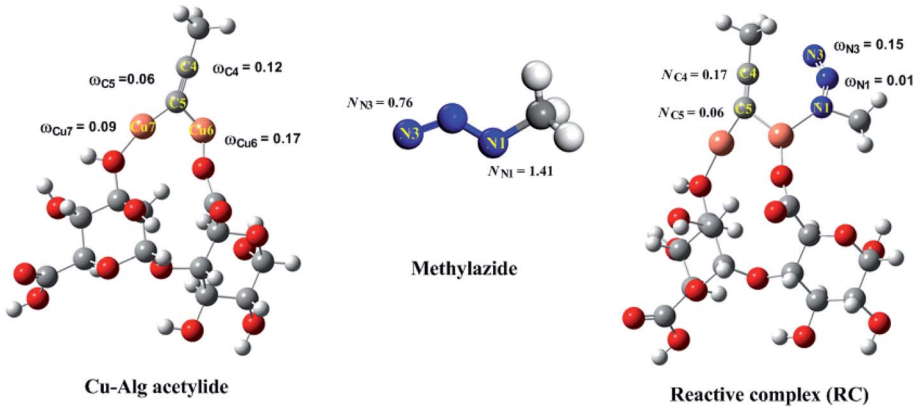

Fig. 8 Local nucleophilicity (N_k) of the azide and local electrophilicity (ω_k) of the reactants, and reactive complex (RC) calculated with the Fukui function.

methyl azide, copper-acetylide and reactive complex (RC) (see Fig. 8). The results indicated that the Cu6 atom was the more electrophilic centre (ω_k) at the copper acetylide intermediate (ω_{Cu6} = 0.17 eV), whereas the N1 nitrogen was the more nucleophilic centre (N_{N1} = 1.41 eV). These findings confirmed that the most favorable single bond formation corresponded to N1 → Cu6, leading to the formation of the reactive complex (RC). The formation of RC is highly exothermic computationally by 3.84 kcal mol^{-1}, using eqn (2) (Fig. S1, see ESI†). Accordingly, the analysis of ω_k and N_k at the RC complex indicates that the C4 and N3 atoms are the most nucleophilic (N_{C4} = 0.17 eV) and most electrophilic (ω_{N3} = 0.14 eV) centres, respectively (Fig. 8). These results show that the most favorable bond formation would correspond to the C4 → N3 pair, which would lead to the formation of the intermediate reaction complex (IC).[82–84] In the next step, a triazolide ligand is formed by reductive elimination, leading to the corresponding 1,4-disubstituted-1,2,3-triazole (Scheme 3). All of the abovementioned results are in agreement with the experimentally observed regioselectivity.[85]

3.4. Recovery and reusability of the catalyst

The recyclability and stability of both Cu(II)-alginate catalysts were also investigated for the reaction of the cycloaddition between phenylacetylene (**1a**) and benzyl azide (**2a**) in water at room temperature (Scheme 2). After completion of the reaction, the reaction mixture was diluted with diethyl ether. The catalyst was then collected by filtration, washed with diethyl ether, dried and used for the next run. In the case of Cu(II)-AHG, it was observed that the catalyst gave a poor yield (*ca.* 30%) after one cycle. Importantly, the catalytic activity and selectivity did not significantly decrease for the next four consecutive uses of the dried Cu(II)-AD beads (Table 4). The structure of the recycled catalyst was investigated by SEM and EDX analysis (Fig. 9 and 10). The SEM analyses of both fresh and recycled catalysts for the Cu(II)-AD beads were almost

Table 4 Recycling of the Cu(II)-AD catalyst

Run	Yield[a] %
1	98
2	89
3	78
4	62

[a] Isolated yield after 48 h.

Open Access Article. Published on 03 September 2020. Downloaded on 2/9/2026 1:57:27 PM.
This article is licensed under a Creative Commons Attribution-NonCommercial 3.0 Unported Licence.

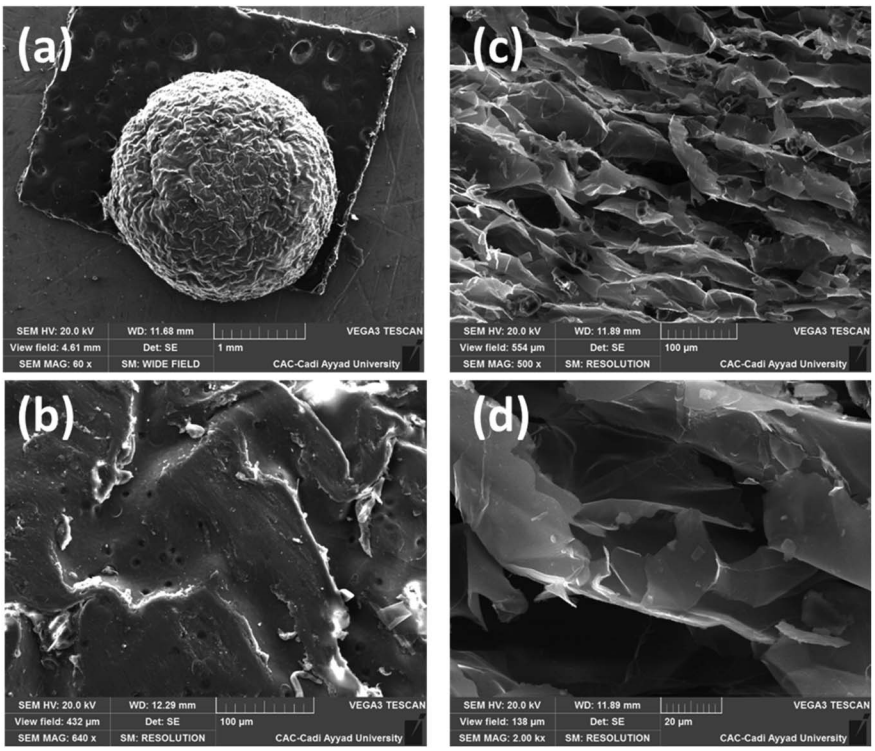

Fig. 9 SEM analysis of the Cu(II)-AD recycled catalyst surface (a and b) and cross-section (c and d).

similar. In addition, the EDX data showed a small decrease in the copper percentage of the catalyst after 4 cycles. After the first run, the copper loading for the reused catalyst was found to be 9.23% (w/w) through atomic absorption spectrometry. The high catalytic activity, simple separation, and recyclability of the Cu(II)-AD hydrogel make this catalyst more environmentally benign.

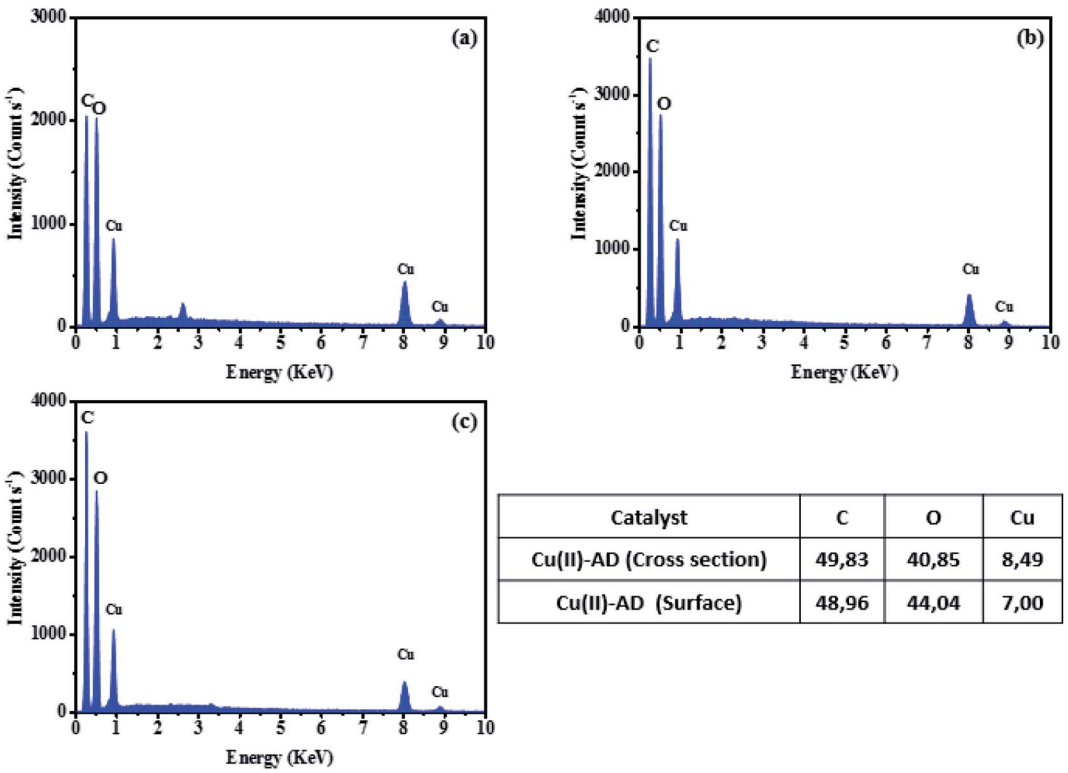

Catalyst	C	O	Cu
Cu(II)-AD (Cross section)	49,83	40,85	8,49
Cu(II)-AD (Surface)	48,96	44,04	7,00

Fig. 10 EDX analysis of the Cu(II)-AD catalyst surface (a), Cu(II)-AD recycled catalyst surface (b), and Cu(II)-AD recycled catalyst cross-section (c).

 This journal is © The Royal Society of Chemistry 2020

Open Access Article. Published on 03 September 2020. Downloaded on 2/9/2026 1:57:27 PM.
This article is licensed under a Creative Commons Attribution-NonCommercial 3.0 Unported Licence.

4. Conclusion

In summary, herein we report the design, preparation and characterization of copper(II)-alginate beads as novel heterogeneous catalysts for the azide–alkyne cycloaddition click chemistry. Cu(II)-alginate hydrogel beads were successfully synthesized through the coordination of copper(II) with the naturally-occurring alginate hydrogel. Different characterization techniques confirmed the immobilization of copper(II) into the alginate hydrogels, influencing the morphology, swelling and thermal properties of the prepared beads as compared to the parent alginate hydrogel. SEM/EDX analyses demonstrated that the Cu(II)-alginate beads exhibited an excellent superporous structure, where the copper(II) ions were homogeneously distributed throughout the hydrogel surface. The prepared catalysts showed high catalytic activity and regioselectivity for the click reaction of 1,4-disubstituted-1,2,3-triazoles in water at room temperature. The catalyst was separated by simple filtration and reused for four cycles of reaction, with a decrease of its catalytic activity and maintenance of their regioselectivity. Moreover, a mechanistic study using DFT calculations allowed for explaining the regioselectivity outcome of the Cu-alginate hydrogel catalysts in the AAC reaction.

Conflicts of interest

There are no conflicts to declare.

Acknowledgements

Financial support from the Ministerio Español de Economía y Competitividad (MINECO) (Project CTQ2016-75068P) is gratefully acknowledged.

References

1 H. C. Kolb, M. G. Finn and K. B. Sharpless, *Angew. Chem., Int. Ed.*, 2001, **40**, 2004–2021.
2 J.-F. Lutz and Nanotechnology for Life Science Research Group, *Angew. Chem., Int. Ed. Engl.*, 2007, **46**, 1018–1025.
3 C. R. Becer, R. Hoogenboom and U. S. Schubert, *Angew. Chem., Int. Ed. Engl.*, 2009, **48**, 4900–4908.
4 C. W. Tornøe, C. Christensen and M. Meldal, *J. Org. Chem.*, 2002, **67**, 3057–3064.
5 V. V. Rostovtsev, L. G. Green, V. V. Fokin and K. B. Sharpless, *Angew. Chem., Int. Ed.*, 2002, **41**, 2596–2599.
6 M. Meldal and C. W. Tornøe, *Chem. Rev.*, 2008, **108**, 2952–3015.
7 M. S. Costa, N. Boechat, É. A. Rangel, F. d. C. da Silva, A. M. T. de Souza, C. R. Rodrigues, H. C. Castro, I. N. Junior, M. C. S. Lourenço, S. M. S. V. Wardell and V. F. Ferreira, *Bioorg. Med. Chem.*, 2006, **14**, 8644–8653.
8 H. Nandivada, X. Jiang and J. Lahann, *Adv. Mater.*, 2007, **19**, 2197–2208.
9 G. C. Tron, T. Pirali, R. A. Billington, P. L. Canonico, G. Sorba and A. A. Genazzani, *Med. Res. Rev.*, 2008, **28**, 278–308.
10 P. Thirumurugan, D. Matosiuk and K. Jozwiak, *Chem. Rev.*, 2013, **113**, 4905–4979.
11 T. Boibessot, D. Bénimèlis, M. Jean, Z. Benfodda and P. Meffre, *Synlett*, 2016, **27**, 2685–2688.
12 A. H. Tarawneh, L. A. A. Al-Momani, F. León, S. K. Jain, A. V. Gadetskaya, S. T. Abu-Orabi, B. L. Tekwani and S. J. Cutler, *Med. Chem. Res.*, 2018, **27**, 1269–1275.
13 V. A. Larionov, H. V. Adonts, Z. T. Gugkaeva, A. F. Smol'yakov, A. S. Saghyan, M. S. Miftakhov, S. A. Kuznetsova, V. I. Maleev and Y. N. Belokon, *ChemistrySelect*, 2018, **3**, 3107–3110.
14 F. J. Smit, R. Seldon, J. Aucamp, A. Jordaan, D. F. Warner and D. D. N'Da, *Med. Chem. Res.*, 2019, **28**, 2279–2293.
15 P. Mathew, A. Neels and M. Albrecht, *J. Am. Chem. Soc.*, 2008, **130**, 13534–13535.
16 D. Mendoza-Espinosa, A. Alvarez-Hernández, D. Angeles-Beltrán, G. E. Negrón-Silva, O. R. Suárez-Castillo and J. M. Vásquez-Pérez, *Inorg. Chem.*, 2017, **56**, 2092–2099.
17 D. Mendoza-Espinosa, R. González-Olvera, G. E. Negrón-Silva, D. Angeles-Beltrán, O. R. Suárez-Castillo, A. Álvarez-Hernández and R. Santillan, *Organometallics*, 2015, **34**, 4529–4542.
18 D. Mendoza-Espinosa, R. González-Olvera, C. Osornio, G. E. Negrón-Silva, A. Álvarez-Hernández, C. I. Bautista-Hernández and O. R. Suárez-Castillo, *J. Organomet. Chem.*, 2016, **803**, 142–149.
19 D. Mendoza-Espinosa, D. Rendón-Nava, A. Alvarez-Hernández, D. Angeles-Beltrán, G. E. Negrón-Silva and O. R. Suárez-Castillo, *Chem.–Asian J.*, 2017, **12**, 203–207.
20 E. Haldón, M. C. Nicasio and P. J. Pérez, *Org. Biomol. Chem.*, 2015, **13**, 9528–9550.
21 A. Mandoli, *Molecules*, 2016, **21**, 1174.
22 L. Liang and D. Astruc, *Coord. Chem. Rev.*, 2011, **255**, 2933–2945.
23 L. Li and Z. Zhang, *Molecules*, 2016, **21**, 1393.
24 A. G. Mahmoud, L. M. D. R. S. Martins, M. F. C. Guedes da Silva and A. J. L. Pombeiro, *Inorg. Chim. Acta*, 2018, **483**, 371–378.
25 A. A. Titov, V. A. Larionov, A. F. Smol'yakov, M. I. Godovikova, E. M. Titova, V. I. Maleev and E. S. Shubina, *Chem. Commun.*, 2019, **55**, 290–293.
26 A. Akbar Khandar, A. Sheykhi, M. Amini, A. Ellern and L. Keith Woo, *Polyhedron*, 2020, **188**, 114698.
27 R. A. Sheldon, I. W. C. E. Arends and U. Hanefeld, in *Green Chemistry and Catalysis*, John Wiley & Sons, Ltd, 2007, pp. 1–47.
28 J. A. Dumesic, G. W. Huber and M. Boudart, in *Handbook of Heterogeneous Catalysis*, American Cancer Society, 2008.
29 A. Schätz, R. N. Grass, W. J. Stark and O. Reiser, *Chem.–Eur. J.*, 2008, **14**, 8262–8266.
30 A. Fihri, D. Cha, M. Bouhrara, N. Almana and V. Polshettiwar, *ChemSusChem*, 2012, **5**, 85–89.
31 N. Madhavan, C. W. Jones and M. Weck, *Acc. Chem. Res.*, 2008, **41**, 1153–1165.
32 S. E. García-Garrido, J. Francos, V. Cadierno, J.-M. Basset and V. Polshettiwar, *ChemSusChem*, 2011, **4**, 104–111.

Open Access Article. Published on 03 September 2020. Downloaded on 2/9/2026 1:57:27 PM.
This article is licensed under a Creative Commons Attribution-NonCommercial 3.0 Unported Licence.

33 K. Y. Lee and D. J. Mooney, *Prog. Polym. Sci.*, 2012, **37**, 106–126.
34 S. N. Pawar and K. J. Edgar, *Biomaterials*, 2012, **33**, 3279–3305.
35 S. Chowdhury, I. R. Chowdhury, F. Kabir, M. A. J. Mazumder, M. H. Zahir and K. Alhooshani, *J. Water Supply: Res. Technol.–AQUA*, 2019, **68**, 369–389.
36 E. M. Ahmed, *J. Adv. Res.*, 2015, **6**, 105–121.
37 H. Omidian, J. G. Rocca and K. Park, *J. Controlled Release*, 2005, **102**, 3–12.
38 L. Bahsis, H. B. El Ayouchia, H. Anane, K. Benhamou, H. Kaddami, M. Julve and S.-E. Stiriba, *Int. J. Biol. Macromol.*, 2018, **119**, 849–856.
39 L. Bahsis, H. B. E. Ayouchia, H. Anane, A. Pascual-Álvarez, G. D. Munno, M. Julve and S.-E. Stiriba, *Appl. Organomet. Chem.*, 2019, **33**, e4669.
40 L. Bahsis, H. B. E. Ayouchia, H. Anane, S. Triki, M. Julve and S.-E. Stiriba, *J. Coord. Chem.*, 2018, **71**, 633–643.
41 M. Fertah, A. Belfkira, E. montassir Dahmane, M. Taourirte and F. Brouillette, *Arabian J. Chem.*, 2017, **10**, S3707–S3714.
42 J. P. Perdew and Y. Wang, *Phys. Rev. B: Condens. Matter Mater. Phys.*, 1992, **45**, 13244–13249.
43 B. Delley, *J. Chem. Phys.*, 1990, **92**, 508–517.
44 B. Delley, *J. Chem. Phys.*, 2000, **113**, 7756–7764.
45 M. Dolg, U. Wedig, H. Stoll and H. Preuss, *J. Chem. Phys.*, 1987, **86**, 866–872.
46 A. Bergner, M. Dolg, W. Küchle, H. Stoll and H. Preuß, *Mol. Phys.*, 1993, **80**, 1431–1441.
47 A. Klamt and G. Schüürmann, *J. Chem. Soc., Perkin Trans. 2*, 1993, 799–805.
48 R. G. Parr, L. v. Szentpály and S. Liu, *J. Am. Chem. Soc.*, 1999, **121**, 1922–1924.
49 L. R. Domingo and P. Pérez, *Org. Biomol. Chem.*, 2011, **9**, 7168–7175.
50 F. De Proft, J. M. L. Martin and P. Geerlings, *Chem. Phys. Lett.*, 1996, **256**, 400–408.
51 J. C. Breger, B. Fisher, R. Samy, S. Pollack, N. S. Wang and I. Isayeva, *J. Biomed. Mater. Res., Part B*, 2015, **103**, 1120–1132.
52 T. T. Le, K. Murugesan, C.-S. Lee, C. H. Vu, Y.-S. Chang and J.-R. Jeon, *Bioresour. Technol.*, 2016, **216**, 203–210.
53 E. G. Deze, S. K. Papageorgiou, E. P. Favvas and F. K. Katsaros, *Chem. Eng. J.*, 2012, **209**, 537–546.
54 N. E. Mousa, C. M. Simonescu, R.-E. Pătescu, C. Onose, C. Tardei, D. C. Culiţă, O. Oprea, D. Patroi and V. Lavric, *React. Funct. Polym.*, 2016, **109**, 137–150.
55 E. Ablouh, A. Essaghraoui, N. Eladlani, M. Rhazi and M. Taourirte, *Water Environ. Res.*, 2019, **91**, 239–249.
56 E. Ablouh, Z. Hanani, N. Eladlani, M. Rhazi and M. Taourirte, *Sustainable Environ. Res.*, 2019, **29**, 5.
57 J. Rui Rodrigues and R. Lagoa, *J. Carbohydr. Chem.*, 2006, **25**, 219–232.
58 K. Akamatsu, K. Maruyama, W. Chen, A. Nakao and S. Nakao, *J. Colloid Interface Sci.*, 2011, **363**, 707–710.
59 Y. Qin, H. Hu and A. Luo, *J. Appl. Polym. Sci.*, 2006, **101**, 4216–4221.
60 K. I. Draget, K. Steinsvåg, E. Onsøyen and O. Smidsrød, *Carbohydr. Polym.*, 1998, **35**, 1–6.
61 J. S. Rowbotham, P. W. Dyer, H. C. Greenwell, D. Selby and M. K. Theodorou, *Interface Focus*, 2013, **3**, 20120046.
62 K. Rajender Reddy, K. Rajgopal and M. Lakshmi Kantam, *Catal. Lett.*, 2007, **114**, 36–40.
63 B. H. Mandal, M. L. Rahman, M. M. Yusoff, K. F. Chong and S. M. Sarkar, *Carbohydr. Polym.*, 2017, **156**, 175–181.
64 R. B. N. Baig and R. S. Varma, *Green Chem.*, 2013, **15**, 1839–1843.
65 H. Ben El Ayouchia, H. ElMouli, L. Bahsis, H. Anane, R. Laamari, C. J. Gómez-García, M. Julve and S.-E. Stiriba, *J. Organomet. Chem.*, 2019, **898**, 120881.
66 S. Pan, S. Yan, T. Osako and Y. Uozumi, *ACS Sustainable Chem. Eng.*, 2017, **5**, 10722–10734.
67 N. Devarajan, M. Karthik and P. Suresh, *Org. Biomol. Chem.*, 2017, **15**, 9191–9199.
68 K. Balaraman and V. Kesavan, *Synthesis*, 2010, **2010**, 3461–3466.
69 C. Iacobucci, S. Reale, J.-F. Gal and F. De Angelis, *Angew. Chem., Int. Ed.*, 2015, **54**, 3065–3068.
70 F. Himo, T. Lovell, R. Hilgraf, V. V. Rostovtsev, L. Noodleman, K. B. Sharpless and V. V. Fokin, *J. Am. Chem. Soc.*, 2005, **127**, 210–216.
71 L. Jin, D. R. Tolentino, M. Melaimi and G. Bertrand, *Sci. Adv.*, 2015, **1**, e1500304.
72 Y.-C. Lin, Y.-J. Chen, T.-Y. Shih, Y.-H. Chen, Y.-C. Lai, M. Y. Chiang, G. C. Senadi, H.-Y. Chen and H.-Y. Chen, *Organometallics*, 2019, **38**, 223–230.
73 R. Roohzadeh, B. Nasiri, A. Chipman, B. F. Yates and A. Ariafard, *Organometallics*, 2019, **38**, 256–267.
74 D. Parasar, T. T. Ponduru, A. Noonikara-Poyil, N. B. Jayaratna and H. V. R. Dias, *Dalton Trans.*, 2019, **48**, 15782–15794.
75 V. O. Rodionov, V. V. Fokin and M. G. Finn, *Angew. Chem., Int. Ed.*, 2005, **44**, 2210–2215.
76 G.-C. Kuang, P. M. Guha, W. S. Brotherton, J. T. Simmons, L. A. Stankee, B. T. Nguyen, R. J. Clark and L. Zhu, *J. Am. Chem. Soc.*, 2011, **133**, 13984–14001.
77 B. T. Worrell, J. A. Malik and V. V. Fokin, *Science*, 2013, **340**, 457–460.
78 C. Nolte, P. Mayer and B. F. Straub, *Angew. Chem., Int. Ed.*, 2007, **46**, 2101–2103.
79 L. R. Domingo, *RSC Adv.*, 2014, **4**, 32415–32428.
80 P. Geerlings, F. De Proft and W. Langenaeker, *Chem. Rev.*, 2003, **103**, 1793–1874.
81 M. J. Aurell, L. R. Domingo, P. Pérez and R. Contreras, *Tetrahedron*, 2004, **60**, 11503–11509.
82 B. F. Straub, *Chem. Commun.*, 2007, 3868–3870.
83 M. Ahlquist and V. V. Fokin, *Organometallics*, 2007, **26**, 4389–4391.
84 V. A. Larionov, A. R. Stashneva, A. A. Titov, A. A. Lisov, M. G. Medvedev, A. F. Smol'yakov, A. M. Tsedili, E. S. Shubina and V. I. Maleev, *J. Catal.*, 2020, **390**, 37–45.
85 H. Ben El Ayouchia, L. Bahsis, H. Anane, L. R. Domingo and S.-E. Stiriba, *RSC Adv.*, 2018, **8**, 7670–7678.

 This journal is © The Royal Society of Chemistry 2020